Atmospheric pollution from shipping and their contributions to air quality degradation in a port site in Shanghai

Xinning Wang[1], Yin Shen[1], Yanfen Lin[1], Jun Pan[1], Yan Zhang[2], Peter K.K. Louie[3], Mei Li[4], Qingyan Fu[1]

[1] Shanghai Environmental Monitoring Center, Shanghai 200030, P.R. China.
[2] Department of Environmental Science and Engineering, Fudan University, Shanghai 200433, P.R. China.
[3] Hong Kong Environmental Protection Department, Hong Kong, P.R. China.
[4] Institute of Mass Spectrometer and Atmospheric Environment, Jinan University, Guangzhou, 510632, China.

Correspondence to: Qingyan Fu (qingyanf@semc.gov.cn)

Abstract. Growing shipping activities in port areas have generated negative impacts on climate, air quality and human health. To better evaluate the environmental impact of ship emissions, in the summer of 2016 ambient air quality measurement was carried out at Shanghai port, one of the busiest ports in the world. The concentrations of gaseous (NO, NO_2, SO_2, O_3) and particulate concentrations ($PM_{2.5}$), particle size distributions and chemical composition of individual ship emission particles were continuously monitored for 3 months. In online measurement the ship emission plumes were clearly distinguishable of both gaseous and particulate matter, which have shown synchronized peaks during plumes. The SO_2 and vanadium particles numbers were found to correlate best with ship emissions in Shanghai port. Single particle mass spectra of fresh ship emission were identified based on the dominant peaks of sulfate, elemental carbon (EC) and indicative metals of V, Ni, Fe and Ca. Temporal trends and size distributions of major ship emission particle types were discussed. The sampled ship emission particles in the port site mainly concentrated in smaller size range where their number contributions are more apparent than their mass. For a costal port close to urban region, the land-based emissions have generated important impacts to the portside air quality, especially for NO_x and $PM_{2.5}$. Quantitative estimation conducted in the present study show that in port region ship emissions contributed 36.4 % SO_2, 0.7 % NO, 5.1 % NO_2, -0.9 % O_3, 5.9 % $PM_{2.5}$, 49.5 % vanadium particles if land-based emissions were included, and 57.2 % SO_2, 71.9 % NO, 30.4 % NO_2, -16.6 % O_3, 27.6 % $PM_{2.5}$, 77.0 % vanadium particles if land-based emissions were excluded.

Keywords

Ship emission; Shanghai port; emission source contribution; SPAMS

1 Introduction

Ship emission constitutes an important source of gaseous and particulate pollution world wide. Growing shipping activities in recent years are attracting much attention to assess its impact on environment and health (Fuglestvedt et al., 2009). For

emissions from sea-going vessels in pristine marine environment, it is found that ship emissions affect clouds properties along cruising route (Petzold et al., 2008;Coggon et al., 2012), which is directly relevant to earth radiation budget and climate issues. In portside or coastal regions, ship emissions generate negative impacts on the air quality at varied degrees (Donateo et al., 2014;Liu et al., 2017). With growing contributions of ship emissions to air pollution, its negative effects on human health of coastal residents is another subject that attracted attentions (Corbett et al., 2007).

The typical fuel that ships burn is Residual Fuel Oil (RFO) with high sulfur content. Combustion of RFO in ship engines produces high concentration of gaseous and particulate pollutants including NOx, SO_2, Elemental Carbon (EC), Organic Carbon (OC), sulfate and trace metals. Emission Factors of these pollutants from various ship types have been determined to develop emission inventories (Moldanova et al., 2013;Buffaloe et al., 2014;Cappa et al., 2014). In ambient measurement, however, the chemical and physical attributes of ship emissions are critical for identifying ship emission and assess their impacts (Murphy et al., 2009). Owing to more stringent regulations against ship emissions by restricting sulfur content in fuel, the detection of ship emissions relying only on individual tracers is unreliable because of the changing composition of RFO in different areas. To better identify ship emission in this context, multi-component characterizations including both gaseous and particulate are necessary in studies of field measurements (Xiao et al., 2018;Viana et al., 2009).

In Yangtze River Delta (YRD) region in China the shipping activities has increased significantly due to intensified international trades in recent years. The accompanying potential environmental and health problems from ship emissions in YRD are well recognized (Chen et al., 2018;Zhang et al., 2017;Fu et al., 2017). Global distributions of ship emission indicate that South and Eastern China Sea regions have the highest pollutants emission densities (Johansson et al., 2017). As shown in an emission inventory in China, shipping traffics emitted about 1.3 Tg SO_2, 1.9 Tg NO_x and 0.16 Tg PM in 2013, with NO_x and PM being equivalent to ~ 34 % and 29 % of total mobile vehicle emissions in China (Fu et al., 2017). To cope with severe air pollution caused by ship emissions, Shanghai government has initiated Domestic Emission Control Areas (DECA) in YRD. At present stage, according to YRD DECA regulations, the sulfur content of any fuel used on board while berthing at Shanghai port shall not exceed 0.5 % (m/m), except for the first hour after arrival and the last hour before departure, which has taken effect on April 1, 2016. This limitation level of sulphur is still higher than the implemented legislation in many harbors/ports in Europe and US (0.1%) (IMO, 2017). The DECA measure was currently implemented mainly in three major shipping areas including PRD, Pearl River Delta - PRD, and Bohai Rim region in China. Efficiency of the ECA measures has been tested in other places (Contini et al., 2015;Merico et al., 2017). It was shown that the control strategies in sulphur in fuel could generate synergetic reduction in both SO_2 and primary PM release from ships. The benefits of DECA measure in YRD were also suggested by the reduction of SO_2 concentration at several monitoring sites in port areas. There is a published study which dealt with the effectiveness of DECA in PRD region, estimating that the DECA measure could result average reduction of 9.54% SO_2 and 2.7% $PM_{2.5}$ in land areas (Liu et al., 2018).

An quantitative estimation of ship emission contribution to air quality is needed for better understanding of its environmental roles and controlling policies. In East Asia, an earlier emission inventory in Shanghai area estimated that the ship emissions were 58160, 51180, 6960 tons/year for NO_x, SO_2 and PM respectively in 2003 (Yang et al., 2007). Over the last decade

Shanghai port throughput of goods has dramatically increased. In 2010, the total ship emissions of NO_X, SO_2 and $PM_{2.5}$ in YRD have grown to 7.1×10^5, 3.8×10^5 and 5.1×10^4 tons/year, respectively (Fan et al., 2016). A more recent study estimated that the primary $PM_{2.5}$ from ships ranged from 0.63 to 3.58 μg/m^3, accounting for 4.23 % of the total $PM_{2.5}$ in Shanghai Port (Zhao et al., 2013), based on a marine port measurement off coast of Shanghai. Such information of port in coastal areas is needed since their closer distance to the urban area of Shanghai city.

In the summer of 2016, an in-site sampling campaign focusing on ship emissions was performed at Shanghai Port. Gaseous and particulate matters concentrations were online monitored for 3 months to identify and characterize the ship emissions in Shanghai port areas. Based on the measurement data, quantitative assessment of the contribution of ship emissions to portside air quality was performed. Ship emission aerosol particles were characterized by a single particle aerosol mass spectrometer (SPAMS) which was deployed at the same site in parallel to the gaseous measurement. The SPAMS was utilized to identify ship emission aerosol composition and size with high temporal resolution, which is useful in detecting fast transient ship plumes, as demonstrated previously (Ault et al., 2010;Healy et al., 2009). In addition, the ship emission particle signatures obtained here is valuable in SPAMS source apportionment in future studies. The present study represents a comprehensive characterization of gaseous and particulate ship emissions in YRD and serves to provide essential scientific supporting information for future evidence-based ship emission control policies.

2 Experimental

2.1 Sampling site

The Waigaoqiao Port (31.337° N, 121.665° E) locates in the northeast of Shanghai city (Fig. 1) and is the largest port in China. The port has about 7 km of docks (3 km north section and 4 km south section). In 2016 the port has yearly traffic of 367 M-tons of goods and container volume of 37.13 million TEU (Twenty-foot Equivalent Unit). Ship categories in port consist of container vessel (62.4 %), tug (18.6 %), oil tanker (9.0 %), bulk (1.8 %), Ro-Ro (1.7 %) and other ships (6.5 %) (private data from authority). A power plant and a shipbuilding factory reside between the north and south section of port, which have their own docks. The portside air monitoring station locates on the south bank of Yangtze River, 400 m away from the nearest dock. Gaseous and particulate matter instruments were installed within the station with the main sampling tube extending through the roof. The outlets of the main sampling tube was 1m above the station roof and 3.5m above the ground. Ship emission plumes could influence the site in wind direction of about 300°-0°-120° sector (Fig. 1). In the summer season the prevailing wind direction of the site is southeast direction. In the supplementary file the wind rose during the sampling period is provided (Fig. S1). In ~55% of time the site was under the impact from port emissions.. To the south and west of site there were intense road traffics of container trucks and the Shanghai outer ring. Traffic emissions in south and west directions have important influences on air pollutions at the monitoring site when inland wind prevails.

2.2 Gaseous, $PM_{2.5}$ and peripheral measurement

The concentrations of gaseous NO-NO_2-NO_x, SO_2, and O_3 were measured continuously from Jun-21 to Sep-21, 2016. The gaseous pollutants were monitored by a suit of Thermal Scientific analyzers (NO-NO_2-NO_x, model 42i; SO_2, model 43i; O_3, 49i) installed in the monitor station. Calibration and checking of instruments were regularly performed by zero checks (through a zero air generator) and span checks (through standard NO_2 and SO_2 gas of known concentrations; the O_3 standard was generated through a calibration photometer system); The $PM_{2.5}$ concentrations were monitored by oscillating microbalance method (Thermo TEOM 1405-F). Calibration of TEOM is not relied on standard, for the aerosol mass on a filter was monitored by the oscillation frequency change of the tapered element over specified time. The regular maintenance of TEOM includes the changing of filters before the filter loading approach 100%. The flow rate of TEOM was checked using a flowmeter. The lower detection limits of these instruments are: 0.4 μg/m^3 (NO, NO_2); 0.5 μg/m^3 (SO_2); 0.5 μg/m^3 (O_3); 1 μg/m^3 ($PM_{2.5}$). Weather conditions (temperature, humidity, pressure, wind speed and direction) were monitored by a mini-weather station installed on the rooftop of the station. The weather station sensor was about 1 m above the station roof and 3.5 m above the ground. Data from all the instruments and the monitor was managed in a customized database and set to 5 min resolution. Atmospheric pollutants concentrations in Shanghai city area, including gaseous pollutants and $PM_{2.5}$ concentrations, were monitored concurrently at 9 national air quality monitoring stations in 1h resolution. The averaged pollutants concentrations at these stations during the sampling period were included for comparison.

2.3 Single particle aerosol mass spectrometer (SPAMS)

During the period from Jun-21 to Sep-21, 2016, a SPAMS (HeXin Analytical Instrument Co., Ltd., China) concurrently characterized single particle chemical composition and size of ambient aerosol in real time (Li et al., 2011). Operation principle of SPAMS is briefly described here. Ambient aerosol is drawn into SPAMS vacuum region through a critical orifice with limited aerosol flow. Aerosol particles then enter an aerodynamic focusing lens (AFL) where they are focused into a thin beam with transiting velocities as a function of particle aerodynamic size. In the SPAMS sizing region particles consecutively encounter two continuous laser beams (532 nm wavelength), reflect light and generate signals in two photomultiplier tubes. The time lag between two PMT signals is used to calculate particle velocity and to trigger the third laser (266 nm wavelength) at appropriate time to ionize the same particle. Chemical composition of ionized particle is measured by a dual polar time-of-flight mass spectrometer to record signal for both negative and positive ions. The time lags between two PMTs of PSL particles of known size are used to calibrate the aerodynamic size of ambient particles. Particle size, dual polar mass spectra, particle reflecting signals from two PMTs are saved for each particle. A $PM_{2.5}$ cyclone was placed at the outlet of sampling tube on the roof of the station to cut out particles larger than 2.5 μm before analysed by SPAMS.

2.4 SPAMS data analysis

The temporal resolution of SPAMS (seconds or minutes) makes it suitable to couple with online gaseous data to identify ship emissions. The quick fluctuations of gaseous concentrations, shifting of wind and the arrival of particle plumes, were well registered in SPAMS data. In addition, present study takes advantage of the power of SPAMS to identify individual ship emission particles based on particle fingerprint. Mass spectral patterns of ship emission particles were firstly identified and then were utilized to extract ship emission particles from single particle dataset. The temporal trends, size distribution, chemical composition, and wind rose of the extracted particles could be examined in further detail.

During sampling of 3 months a large amount of particles were chemically analysed by SPAMS (>2.3 million mass spectra). The identification of ship emission particles from 2.3 million total particles were based on a combined method of peak searching and algorithm clustering. Specifically, the SPAMS data are pre-analysed by visually inspecting of individual particle mass spectra to identify MS patterns during ship plumes. The concurrent SO_2 concentrations were utilized to locate ship emission plumes when sharp SO_2 peaks occurred, which is typical for RFO combustions (Murphy et al., 2009;Merico et al., 2016). Compared with non-plumes period, the most important indicating peaks occurred at V^+(51), VO^+(67), Fe^+(56), Ni^+(58) and serial peaks of elemental carbon at C_n^+(n=1,2,3…,12) in the positive mass spectrum (Ault et al., 2010;Healy et al., 2009;Ault et al., 2009). In this study the vanadium mass peaks (peak V^+(51) and VO^+(67))) were determined to be a prerequisite to indicate ship particles during plumes. Further notes on this particle identification method from ship emission are seen in the supplementary material. Peak searching method of criteria of m/z = 51 and 67 (i.e., only the existence of mass peak at 51 and 67, no peak area limitation) was firstly applied to search all possible candidates from all analysed particles. This search criterion is not too stringent because particles producing organic peaks at the same nominal mass (e.g. $C_4H_3^+$(51), $C_4H_3O^+$(67)) could interfere and may enter into searched clusters. Then the ART-2a algorithm (Song et al., 1999) was applied to the searched clusters to generate sub-clusters of particles (Vigilance=0.85; Learning=0.05; Iteration=20). By inspecting composition, size and wind rose patterns of sub-clusters, a small fraction of outlier particles from non-shipping emission sources were thus picked out and discarded.

2.5 Evaluation of ship emission contribution

The calculations method of ship emission contributions used in this study, which was originally developed by (Contini et al., 2011), is based on the extraction of ship emission plumes from background concentrations of pollutants :

$$\varepsilon_A = \frac{\Delta C_A F_{plm}}{C_A}$$

Where: ε_A, ship emission contributions of pollutants A; ΔC_A, the difference between average concentrations during plumes and non-plumes; F_{plm}, fraction of cases of plumes; C_A, the average concentration of pollutant A during reference period. The uncertainties of ε_A determined in this method could arise from several factors, such as the definition of port direction sector, the definition of plumes (the threshold level that discriminate plumes and the background), and pollutants and wind field

measurements. This study estimate the uncertainties by subjecting ε_A to the slight adjustment of the port directions by ±10° and pollutants threshold levels by 20% to inspect its variations. To conform to the original work (Contini et al., 2011), calm wind periods (wind speed < 0.5 m/s) were considered in the evaluation of uncertainties (either excluding or including calm wind periods).

3 Results and discussions

3.1 Identification and statistics of ship emission plumes

In the vicinity of port, the measured ship emitted pollutants often produce sharp peaks in relatively short period (Fig. 2). The sharp peaks are caused by ship emission plumes corresponding to shipping activities such as arrival, hoteling and departure, which typically persist for a few (mostly 3-6) hours. The measured SO_2, NO, NO_2, O_3 and $PM_{2.5}$ concentrations during a typical period (Aug 27-29) are shown in Figure 2 to illustrate several cases. For comparison the averaged SO_2 concentration in Shanghai city and vanadium particle number concentration during the same period are included. It is clear that during plumes tracking period, the SO_2 concentration peaks were well correlated with vanadium particles number as detected by SPAMS. The synchronous peaks of gaseous and particulate matters during plumes was similarly observed elsewhere (Healy et al., 2009;Ault et al., 2010;Merico et al., 2016). Wind field during plumes also support they were actual emission plumes arrived at the site (Fig. 2).

The measured gaseous and particulate matters demonstrated different characters during sampling period. In most cases of the non-plume periods the portside SO_2 concentration matched well with the SO_2 in Shanghai city. This is a suggestion that a background SO_2 concentration of regional scale is underlying the measured concentration in portside, upon which the local SO_2 plumes were superimposing. As two typical combustion products, the NO and NO_2 concentrations also show corresponding elevated concentrations during plumes under favourable wind fields (Fig. 2). However, during the whole study NO and NO_2 are more importantly influenced by land-based traffics (mostly from transportation diesel trucks) when the inland wind prevails. The ship emission NO_x plumes reached sampling site have been slightly aged. To understand the aging effect, when wind direction is in port sector (300°-0°-120°), the averaged NO/NO_2 ratio is 0.6 (mostly fall in 0.1~4.5 range), lower than typical ratio of 4 at ship exhaust (Alföldy et al., 2013) , suggesting the oxidation of primary NO into NO_2 had occurred for some time (1~50 min, based on wind speed measurement and transportation distance). This result is evidenced by the apparent consumption of O_3 in plumes as shown in Figure 2, commonly termed as titration effect between NO_x and O_3. The $PM_{2.5}$ mass concentration did not show as apparent response as that of SO_2 during ship emission plumes, despite that the typical vanadium particles had reached the site, as shown. The obscure response of $PM_{2.5}$ during ship plumes is explained by the finer particle sizes in relatively fresh ship emissions, as discussed subsequently.

Considering the facts described above, the present study defines ship plume periods by using SO_2 concentrations and vanadium particle number concentrations. For SO_2, a minimum threshold of Δ_{SO2} = SO_2(Port) - SO_2(Shanghai) > 5 ug/m^3 is applied to indicate ship plumes. For ship emission particles, the number concentration of vanadium particle is considered because in

some cases the SO_2 peaks are absent or obscure as typical fresh vanadium particles are indeed mount up quickly. The occurrence probability of this kind of event is low (3% in cases). The causes of this kind of events are two-fold: firstly, it is maybe due to the anchored ships burning low sulfur content oil (<0.5 % m/m) to comply with regulations in the port region, which came into force on April 1, 2016; secondly, it is also possible that the vanadium particles be emitted from industry sources such as petroleum refinery companies in this region. The wind directions when these events happened support both of the proposed causes. In this study the threshold of vanadium particle detection speed in ship plumes are set to $C_V > 25$ particles/hour. That is, ship plumes are defined as either $\Delta_{SO2} > 5\mu g/m^3$ or $C_V > 25$ particles/hour.

There were about 210 ship emission plumes captured during the sampling campaign. Table 1 summarizes the statistics on the concentrations of SO_2, NO, NO_2, O_3, $PM_{2.5}$ in port area and Shanghai city during the sampling period. Vanadium particles number concentrations are represented by particle detection speeds by SPAMS. It is stated that the SPAMS detection speed are positively correlated with particle number concentrations in ambient air, but should not be explained as absolute number concentrations without correction for SPAMS efficiency (Wenzel et al., 2003). Statistics are performed on pollution level in plume periods and in non-plumes. To separate influences from land sources (principally traffics), non-plume periods during wind from port direction are calculated in Table 1.

In general, the port site has concentrations of combustion products SO_2 and NO_x much higher than that in Shanghai city regions (Table 1). For SO_2 its concentrations in non-plumes were comparable with that in Shanghai city, regardless of wind direction, representing a background SO_2 level. However, NO_X concentrations in non-plumes from port sector wind were significantly lower than from land directions. This result suggests a larger ship emission contribution to portside SO_2 than to NO_x. For NO_x, due to the specific geographic proximity of Waigaoqiao port, its concentration was more importantly impacted by land-based traffics. In general the ozone concentrations in port were lower than Shanghai urban region by 13-33 %. The lower O_3 level around portside is consistent with higher SO_2 and NO_x concentrations in this area to consume O_3. For $PM_{2.5}$, its concentrations in port area are slightly lower than Shanghai city either in plume or non-plume periods, although vanadium particles concentrations in plumes were about 4 times higher than in non-plumes (Table 1). Longer period of $PM_{2.5}$ data at the same station supports the lower $PM_{2.5}$ concentration compared to Shanghai city, suggesting that it is a general trend at this port site. This is probably caused by the clean air advection from the sea and the wiping out effect of adjacent water surface through particle sedimentation. The vanadium particle detection probability, measured as the number fraction in total particles, is clearly larger (6.7 % on average) in portside than the urban area in Shanghai (1-2 %) (Liu et al., 2017).

3.2 Particles properties from ship emission

3.2.1 Discrimination of fresh and background ship emission particles in port site

In single particle characterization techniques, fresh or 'pure' ship emission particles is separable from background or aged aerosol based on single particle signatures. The mass spectra of fresh and aged ship emission particles, wind roses and size distributions are shown in Figure 3, 4. It was observed that particles from ship emission plumes were characterized by the

absence of or very low nitrate (-62NO_3 in negative spectra) signal in mass spectra, a pattern commonly found in combustion source characterizations (Spencer et al., 2006;Toner et al., 2006). In another respect, the temporal pattern, wind rose and size of nitrate containing vanadium particles were disproportionately distributed compared with fresh ones, which distinguished themselves as background ship emission particles (Healy et al., 2009;Ault et al., 2010) (Fig. 3). The dominant peaks in mass spectra of fresh ship emission particles are sulfate (-97HSO_4^-), EC (C_n^+/C_n^-, n are integers), and vanadium (51V^+, 67VO^+) peaks, indicating the major components found in ship emission particles (Moldanova et al., 2013;Becagli et al., 2012;Murphy et al., 2009). Except for the nitrate peak (-62NO_3^-), other mass spectral patterns of background and fresh ship emission particles are similar (Fig. 3). Although organics is an important component of ship emission particles (Lack et al., 2009), the organic mass peaks in SPAMS spectra are insignificant compared with metal and EC peaks as shown in Fig. 3. The Lower OC signal is owing to the fact that SPAMS is not so sensitive to organics due to the low ionization efficiencies in laser ionization (Ulbrich et al., 2009). However, an cluster of organic particles were indeed identified in ship plumes, although of minor detection probability, as discussed subsequently in 3.2.2.

Wind roses and size distributions of fresh and aged ship emission particles were also distinguishable. The fresh vanadium particles have wind rose pattern running parallel with the direction of riverbanks (300°-0°-120°). This is strong evidence that ships are the most predominant source of fresh vanadium particles in Shanghai port. Background vanadium particles, however, did not show any prominent source directions and displayed nearly uniform distributions in all directions. It is assumed that the aged vanadium particles are background particles which have undergone atmospheric processing in local or regional scale. The size distributions of vanadium particles as shown in Figure 4 indicates fresh vanadium particles with dominate particle numbers in smaller size range (<0.5 μm), compared with background ones. Although SPAMS detection efficiency declines in this size range due to the because of the smaller section to reflect laser light, significant number of ship emission particles were still detected in this size range. The explanation is that these particles are non-spherical fractal agglomerates, such as EC particles, having significantly larger cross sections to reflect laser light and be detected in SPAMS. The non-spherical fractal shape of fresh vanadium particles is seen with soot particle from fresh combustion sources. Similar observations were reported in other studies using single particle mass spectrometer in ultra-fine size range (Ault et al., 2010).

3.2.2 Particle types in fresh ship emission plumes

The major particle types of fresh ship emission particles were identified after the separation of background particles. The composition, size distributions and emission characters were analysed to obtain the further information of these types, which will be helpful to in particle source identification in other sites. In general, the fresh vanadium particles could be grouped into 4 types based on their chemical composition: V-OC, V-EC, V-ECFe and V-Ash, and the average mass spectra are shown in Figure 5. The negative mass spectra of the four types were similar in that the SO4 peak were dominant in addition to other negative EC peaks, which is consistent with the elevated SO2 concentrations in plumes. The major chemical differences of the four particle types are in the positive mass spectra as depicted in Figure 5. In the positive mass spectra the V-OC type are characterized by the dominant organic peaks like $C_2H_3^+$, $C_2H_5^+$, $C_2H_3O^+$, with non or insignificant EC peaks. Generally the

organics are ionized in low efficiencies in SPAMS. The rich organic signals of V-OC particles indicate that they are mainly composed of organics in engine exhaust plumes (Lack et al., 2009;Moldanova et al., 2013). The V-EC particles produce dominant EC peaks from C_1^+ to C_{13}^+ and metal peaks of V and Na, but without iron peaks Fe^+. This type is also the most abundant type of all vanadium particles. The V-ECFe type is similar to V-EC except for the addition of Fe^+ and Ca^+, Ni^+ peaks of lower frequencies. The V-Ash particles produce minor or no EC peaks except some metal peaks of V, Fe and Ni in positive spectra. These metals are used as lubricant additives or inherently present in RFO, therefore their presence in ship emission particles are expected and commonly found (Becagli et al., 2012;Moldanova et al., 2013).

Temporal concentrations and size distributions of these particle types are shown in Figure 6. Temporal number concentrations of these particle types displayed daily variations, with higher concentrations in daytime than night. The temporal concentrations of these particle types were poorly correlated (R^2<0.4), suggesting they were emitted differently. Since these particles were detected in a portside environment, they were assumed to be emitted by ships of different engine types or modes of operation. The V-OC particles, although having low ionization probabilities, were found to concentrate in specific cases of plumes. Since the information of individual ships is not yet available, it is therefore not attempted to link V-OC particle plumes to specific ship types directly in the present study. The V-OC particles concentrated in specific ship emission plumes and its' number concentration peaks were usually narrower (~ 1 hour) than the other particle types (3~5 hour). Sizes of V-OC particles were more uniformly distributed as compared with the other types (Fig. 6). Similar organic-rich particles were identified from ship exhaust by other technique (Moldanova et al., 2013).

The V-EC particles dominated the particle numbers in ship plumes in this study. Compared with the other types their sizes enriched in smaller size ranges (< 0.5 μm), which is a typical character of soot particles from the combustion of RFO (Moldanova et al., 2013). The V-Ash particles, which is most probably the ash spheres from combustion process of inorganic constituents in RFO and lubricants, are mainly detected in larger size range (> 0.5 μm) (Fig. 6). SPAMS measure particle aerodynamic size which is both determined by particle size and density. The larger densities of metal oxides or salts in V-Ash particles, as compared with soot agglomerates, is also making contributions in its size distribution. The origin of V-ECFe types were ~~are~~ probably the result of internal mixing between V-EC and V-Ash particles. Their size distribution is more similar to V-Ash type.

3.3 Contributions of ship emission to ambient pollutants in port area

For a coastal port, the evaluation of ship emission to air quality needs to identify impacts from land-based emissions. Obviously these land-based emissions are making greater influences to portside air quality than a marine port far from coast (Zhao et al., 2013). To give an intuitive illustration, the averaged concentrations of SO_2, O_3, NO, NO_2, $PM_{2.5}$ and vanadium particle numbers in different wind directions are summarized in Figure 7. Concentrations of pollutants has demonstrated varied dependency on local wind conditions. It is evident that, for the coastal port site in this study, the NO_x and $PM_{2.5}$ concentrations, were highest during land direction wind prevails. As a contrast the SO2 concentrations and vanadium particle numbers were dominant only when winds from port sectors. The hotspots in wind rose of vanadium particle are most probably produced by individual docks

along the riverside. The wind dependence of ozone concentrations is less apparent, except its' depletion in regions of high NO_x and SO_2 levels in wind roses, as previously explained. Obviously the port site was receiving very different pollution impacts from land emission and the ship emissions in port. Present study tries to separate land-based emission influences by limiting wind directions only in port directions. In the calculation of ship emission contribution, two reference periods were considered in this study: the entire study period (irrespective of wind) and only when the site was in downwind directions of port.

Ship emission contributions of measured respective pollutants in two reference periods are summarized in Table 2. Results show that, if the land-based emissions were considered, the relative contributions from ship emission for SO_2 (36.4 %) were much higher than for NO (0.7 %), NO_2 (5.1 %), and $PM_{2.5}$ (5.9 %). The low contributions of NO_x are due to the inclusion of traffic emissions of stronger intensities in the land directions. The main sources of NOx in land directions was considered not far from the site because the average NOx levels in Shanghai city is lower than the port site, as evidenced in Table 1. In the port site the vanadium particle number concentrations (PNC_v) were dominantly contributed (49.5 %) by ship emissions. The PNCv contribution is a lower estimation considering that SPAMS detect particles less efficiently for smaller particles, where the vanadium particles tend to concentrate. Contributions of PNC_v in different particle size ranges were also calculated in table 2. In either of reference periods (excluding or including land-based emissions), ship emission contributions to PNC_v in smaller size range (0-0.4μm) are larger compared with PNC_v in larger size ranges (0.4-0.8 μm, 0.8-2.5μm).

The relative contributions of PNC_v from ship emission is apparently higher than $PM_{2.5}$ on mass concentration. Previous study showed that the direct $PM_{2.5}$ contribution from ship traffics lies within 1-8% range (Contini et al., 2011;Contini et al., 2015). Recent studies carried in Mediterranean region found that ship emission contributed 0.3-7.4% $PM_{2.5}$ concentrations in port areas (Merico et al., 2016). Ship emission studies in Europe and other regions was reviewed, and its concluded that shipping traffics contributions to $PM_{2.5}$ were in 1-14% range, with higher contributions with decreasing particle size (Viana et al., 2014). The calculated value of $PM_{2.5}$ in the present site is within the reported ranges. Recently (Merico et al., 2017) compared ship traffic atmospheric impacts using inventories, experimental data and modelling approaches in Adriatic-Ionian port areas, and found that ships contributed 0.5-7.4% $PM_{2.5}$ in these areas. The same study further found that ship traffics contribution to particle number concentrations (PNC) is 2-4 time larger than mass concentrations of $PM_{2.5}$. The PNC is not currently measured, instead the size distributions, PNC contributions of vanadium particles in different sizes, as measured by SPAMS, apparently agrees with these previous work.

In a study carried out at Yangshan marine port of Shanghai, the calculated $PM_{2.5}$ contribution (~4 %) is smaller than present study (5.9 %) (Zhao et al., 2013). In this study a different method was used to evaluate ship emissions, relying on vanadium concentrations to indicate ship emissions. Considering the methodology differences, it is deemed that the results from the two studies are similar within the uncertainty range (Table 2). A previous estimation in Shanghai area using inventories method showed that ship emissions contributed 9 % NO_x and 5.3 % $PM_{2.5}$ in Shanghai area (Zhang et al., 2017), generally agrees with this study in the condition of including land-based emissions (Table 2). However, for SO_2 the contribution in that estimation (12 %) is significantly smaller than the 36.4 % in this study. The high SO_2 levels in this study is a local character of the port site which is close to emission sources. After transported to the urban region the high SO_2 concentrations will dissipate and

strength weakened. It is noted that, the synchronized SO_2 and vanadium particles plumes as observed in the port site, are observed in a much less frequency in a urban cite in Shanghai city where another SPAMS is monitoring. Estimation of ship emission impacts to the urban area will be the subject of future studies.

By limiting the sampling with time windows to periods during winds from port sector, the influences of land-based emissions could be largely eliminated. As shown in table 2, by considering port sector wind, for all pollutants the ship emission contributions were magnified in amplitude. The most significant change occurs for gaseous NO_x, whose contributions from ship emission increased to levels larger or comparable with SO_2. Contributions obtained here can be compared with a similar study carried out in a European port (Merico et al., 2016). Gaseous emissions of NO, NO_2 and SO_2 were similar between these two studies, which is impressive considering the larger throughput of goods in Shanghai port. However, in an absolute sense, this study estimate that ship emissions contribute to 5.68 $\mu g/m^3$ SO_2, 3.00 $\mu g/m^3$ NO_x and 1.57 $\mu g/m^3$ $PM_{2.5}$ during the sampling period. These values are comparable or higher than the reported results in ports in other regions (Viana et al., 2014). For example, a previous study found that the ship emitted particles contributed 0.8 $\mu g/m^3$ (primary particles) and 1.7 $\mu g/m^3$ (secondary particles) in Bay of Algeciras (Viana et al., 2009). Due to the adjacency of the site to port, the calculated $PM_{2.5}$ contribution could be largely deemed as primary for present site. The relative contributions of pollutants are partly compensated by the higher background pollution levels in this region.

4 Conclusions

In the summer of 2016, an experimental study was carried out to characterize and quantify ship emissions in the Shanghai port. Obvious ship emission plumes were detected in the port site through online measurement of gaseous and particulate matter. During plumes the SO_2 and vanadium particles concentrations has demonstrated well synchronized peaks, which could be reliably used to indicate the arrival of ship emission plumes. Statistics of pollutants during plumes show that the concentrations of SO_2 in plumes are about 3 times higher than the background concentrations. Except the plume periods, the SO_2 concentrations in port site varies with the background SO_2 level in regional scale. NO_x emissions from ships were also obvious during plumes, however, its' concentrations in port site are under much stronger influences from land emissions. For particulate matters, the primary ship emission produce dominant vanadium particle number concentrations (PNC_v) to the portside while its' contribution to the mass concentrations ($PM_{2.5}$) was less significant. Other pollutants O_3 was depleted by elevated primary NO_x and SO_2 emissions in port regions, resulting 11-33 % ozone consumption compared with urban region of Shanghai.

Particle size distributions and chemical composition of individual ship emission particles were identified by single particle mass spectrometry at the same site. Similar as SO_2, the ship emission particles in portside could also be grouped into freshly emitted and background particle types. The mass spectra of fresh ship emission particles contain dominant peaks of EC, sulfate and trace metals (V, Ni, Fe and Ca). Size distribution of ship emission particles showed that they are tend to concentrate in smaller size range (< 0.5 μm), which is most probably composed of fractal black carbon agglomerates. Based on the different

chemical composition of ship emission particles, ship emission particles during plumes could be grouped into four major types: V-OC, V-EC, V-ECFe and V-Ash. These particles were shown to reserve different temporal and size distribution trends.

Ship emission contributions to the air quality in Shanghai port area was quantified by extracting pollution concentrations during plume periods. The contributions of ship emissions were evaluated in two scenarios where the land-based emission sources are either included or excluded. Results show that ship emission was a major contributor to the ambient SO_2 (5.68 $\mu g/m^3$, 36.4%) and vanadium particle concentrations (49.5%) in port side. NO_x contribution (3.00 $\mu g/m^3$, 5.8%) from shipping emissions was insignificant compared with emission from land-based sources, which was mainly from transportation sources. If land sources were excluded, shipping relative contributions of NO_x became comparable with that of SO_2. Due to the high NO_x and SO_2 levels in this area, significant fraction of ozone concentration was found to be depleted. Primary particles from ship emission were estimated to contribute to 5.9% (1.57 $\mu g/m^3$) $PM_{2.5}$ concentration during the sampling period. In the sense of particle number concentration (PNC), over 44% vanadium PNC in the port site were found to be contributed by ship emission. The vanadium PNC contribution from ship emission were found to increase with decreasing particle size, with 57% vanadium particles smaller than 0.4μm were found to sourced from ship emission. Since the size and mass of fresh exhaust particles are small, the mass concentration PM from exhaust pipes would be inappropriate to represent their real mass contribution after atmospheric aging. This study supports that particle number concentration (PNC) be included to fully characterize primary ship emitted particles.

Disclaimer

The content of this paper does not necessarily reflect the views and policies of the HKSAR Government, nor does mention of trade names or commercial products constitute an endorsement or recommendation of their use.

Acknowledgement

This work was financially supported by the Shanghai Science and Technology Committee (STCSM) projects (Grant No. 15DZ1205402 and 17DZ1203100). Analysis of SPAMS data was funded by National Natural 422 Science Foundation of China (Grant No.21607056). Special thanks are addressed to Shanghai East Container Terminal Co., Ltd. (SECT) for their valuable aids during observations, and Shanghai Environmental Monitoring Technology and Appliance Ltd. for attentive instrument maintenance services in the campaign.

References

Agrawal, H., Welch, W. A., Henningsen, S., Miller, J. W., and Cocker, D. R., III: Emissions from main propulsion engine on container ship at sea, Journal of Geophysical Research-Atmospheres, 115, 10.1029/2009jd013346, 2010.

Alföldy, B., Lööv, J. B., Lagler, F., Mellqvist, J., Berg, N., Beecken, J., Weststrate, H., Duyzer, J., Bencs, L., Horemans, B., Cavalli, F., Putaud, J. P., Janssens-Maenhout, G., Csordás, A. P., Van Grieken, R., Borowiak, A., and Hjorth, J.: Measurements of air pollution emission factors for marine transportation in SECA, Atmos. Meas. Tech., 6, 1777-1791, 10.5194/amt-6-1777-2013, 2013.

Aulinger, A., Matthias, V., Zeretzke, M., Bieser, J., Quante, M., and Backes, A.: The impact of shipping emissions on air pollution in the greater North Sea region - Part 1: Current emissions and concentrations, Atmospheric Chemistry and Physics, 16, 739-758, 10.5194/acp-16-739-2016, 2016.

Ault, A. P., Moore, M. J., Furutani, H., and Prather, K. A.: Impact of Emissions from the Los Angeles Port Region on San Diego Air Quality during Regional Transport Events, Environmental Science & Technology, 43, 3500-3506, 10.1021/es8018918, 2009.

Ault, A. P., Gaston, C. J., Wang, Y., Dominguez, G., Thiemens, M. H., and Prather, K. A.: Characterization of the Single Particle Mixing State of Individual Ship Plume Events Measured at the Port of Los Angeles, Environmental Science & Technology, 44, 1954-1961, 10.1021/es902985h, 2010.

Becagli, S., Sferlazzo, D. M., Pace, G., di Sarra, A., Bommarito, C., Calzolai, G., Ghedini, C., Lucarelli, F., Meloni, D., Monteleone, F., Severi, M., Traversi, R., and Udisti, R.: Evidence for heavy fuel oil combustion aerosols from chemical analyses at the island of Lampedusa: a possible large role of ships emissions in the Mediterranean, Atmospheric Chemistry and Physics, 12, 3479-3492, 10.5194/acp-12-3479-2012, 2012.

Buffaloe, G. M., Lack, D. A., Williams, E. J., Coffman, D., Hayden, K. L., Lerner, B. M., Li, S. M., Nuaaman, I., Massoli, P., Onasch, T. B., Quinn, P. K., and Cappa, C. D.: Black carbon emissions from in-use ships: a California regional assessment, Atmospheric Chemistry and Physics, 14, 1881-1896, 10.5194/acp-14-1881-2014, 2014.

Cappa, C. D., Williams, E. J., Lack, D. A., Buffaloe, G. M., Coffman, D., Hayden, K. L., Herndon, S. C., Lerner, B. M., Li, S. M., Massoli, P., McLaren, R., Nuaaman, I., Onasch, T. B., and Quinn, P. K.: A case study into the measurement of ship emissions from plume intercepts of the NOAA ship Miller Freeman, Atmospheric Chemistry and Physics, 14, 1337-1352, 10.5194/acp-14-1337-2014, 2014.

Chen, D., Zhao, N., Lang, J., Zhou, Y., Wang, X., Li, Y., Zhao, Y., and Guo, X.: Contribution of ship emissions to the concentration of PM2.5: A comprehensive study using AIS data andWRF/Chemmodel in Bohai Rim Region, China, Science of the Total Environment, 610, 1476-1486, 10.1016/j.scitotenv.2017.07.255, 2018.

Coggon, M. M., Sorooshian, A., Wang, Z., Metcalf, A. R., Frossard, A. A., Lin, J. J., Craven, J. S., Nenes, A., Jonsson, H. H., Russell, L. M., Flagan, R. C., and Seinfeld, J. H.: Ship impacts on the marine atmosphere: insights into the contribution of

shipping emissions to the properties of marine aerosol and clouds, Atmospheric Chemistry and Physics, 12, 8439-8458, 10.5194/acp-12-8439-2012, 2012.

Contini, D., Gambaro, A., Belosi, F., De Pieri, S., Cairns, W. R. L., Donateo, A., Zanotto, E., and Citron, M.: The direct influence of ship traffic on atmospheric PM2.5, PM10 and PAH in Venice, Journal of Environmental Management, 92, 2119-2129, 10.1016/j.jenvman.2011.01.016, 2011.

Contini, D., Gambaro, A., Donateo, A., Cescon, P., Cesari, D., Merico, E., Belosi, F., and Citron, M.: Inter-annual trend of the primary contribution of ship emissions to PM2.5 concentrations in Venice (Italy): Efficiency of emissions mitigation strategies, Atmospheric Environment, 102, 183-190, 10.1016/j.atmosenv.2014.11.065, 2015.

Corbett, J. J., Winebrake, J. J., Green, E. H., Kasibhatla, P., Eyring, V., and Lauer, A.: Mortality from ship emissions: A global assessment, Environmental Science & Technology, 41, 8512-8518, 10.1021/es071686z, 2007.

Donateo, A., Gregoris, E., Gambaro, A., Merico, E., Giua, R., Nocioni, A., and Contini, D.: Contribution of harbour activities and ship traffic to PM2.5, particle number concentrations and PAHs in a port city of the Mediterranean Sea (Italy), Environmental Science and Pollution Research, 21, 9415-9429, 10.1007/s11356-014-2849-0, 2014.

Fan, Q., Zhang, Y., Ma, W., Ma, H., Feng, J., Yu, Q., Yang, X., Ng, S. K. W., Fu, Q., and Chen, L.: Spatial and Seasonal Dynamics of Ship Emissions over the Yangtze River Delta and East China Sea and Their Potential Environmental Influence, Environmental Science & Technology, 50, 1322-1329, 10.1021/acs.est.5b03965, 2016.

Fu, M., Liu, H., Jin, X., and He, K.: National- to port-level inventories of shipping emissions in China, Environmental Research Letters, 12, 10.1088/1748-9326/aa897a, 2017.

Fuglestvedt, J., Berntsen, T., Eyring, V., Isaksen, I., Lee, D. S., and Sausen, R.: Shipping Emissions: From Cooling to Warming of Climate-and Reducing Impacts on Health, Environmental Science & Technology, 43, 9057-9062, 10.1021/es901944r, 2009.

Gonzalez, Y., Rodriguez, S., Guerra Garcia, J. C., Luis Trujillo, J., and Garcia, R.: Ultrafine particles pollution in urban coastal air due to ship emissions, Atmospheric Environment, 45, 4907-4914, 10.1016/j.atmosenv.2011.06.002, 2011.

Healy, R. M., O'Connor, I. P., Hellebust, S., Allanic, A., Sodeau, J. R., and Wenger, J. C.: Characterisation of single particles from in-port ship emissions, Atmospheric Environment, 43, 6408-6414, 10.1016/j.atmosenv.2009.07.039, 2009.

Johansson, L., Jalkanen, J.-P., and Kukkonen, J.: Global assessment of shipping emissions in 2015 on a high spatial and temporal resolution, Atmospheric Environment, 167, 403-415, 10.1016/j.atmosenv.2017.08.042, 2017.

IMO: Emission Control Areas (ECAs) designated under MARPOL Annex VI, 2017.

Jonsson, A. M., Westerlund, J., and Hallquist, M.: Size-resolved particle emission factors for individual ships, Geophysical Research Letters, 38, 10.1029/2011gl047672, 2011.

Lack, D. A., Corbett, J. J., Onasch, T., Lerner, B., Massoli, P., Quinn, P. K., Bates, T. S., Covert, D. S., Coffman, D., Sierau, B., Herndon, S., Allan, J., Baynard, T., Lovejoy, E., Ravishankara, A. R., and Williams, E.: Particulate emissions from commercial shipping: Chemical, physical, and optical properties, Journal of Geophysical Research-Atmospheres, 114, 10.1029/2008jd011300, 2009.

Li, L., Huang, Z., Dong, J., Li, M., Gao, W., Nian, H., Fu, Z., Zhang, G., Bi, X., Cheng, P., and Zhou, Z.: Real time bipolar time-of-flight mass spectrometer for analyzing single aerosol particles, International Journal of Mass Spectrometry, 303, 118-124, https://doi.org/10.1016/j.ijms.2011.01.017, 2011.

Liu, H., Jin, X., Wu, L., Wang, X., Fu, M., Lv, Z., Morawska, L., Huang, F., and He, K.: The impact of marine shipping and its DECA control on air quality in the Pearl River Delta, China, Science of The Total Environment, 625, 1476-1485, https://doi.org/10.1016/j.scitotenv.2018.01.033, 2018.

Liu, Z., Lu, X., Feng, J., Fan, Q., Zhang, Y., and Yang, X.: Influence of Ship Emissions on Urban Air Quality: A Comprehensive Study Using Highly Time-Resolved Online Measurements and Numerical Simulation in Shanghai, Environmental Science & Technology, 51, 202-211, 10.1021/acs.est.6b03834, 2017.

Merico, E., Donateo, A., Gambaro, A., Cesari, D., Gregoris, E., Barbaro, E., Dinoi, A., Giovanelli, G., Masieri, S., and Contini, D.: Influence of in-port ships emissions to gaseous atmospheric pollutants and to particulate matter of different sizes in a Mediterranean harbour in Italy, Atmospheric Environment, 139, 1-10, 10.1016/j.atmosenv.2016.05.024, 2016.

Merico, E., Gambaro, A., Argiriou, A., Alebic-Juretic, A., Barbaro, E., Cesari, D., Chasapidis, L., Dimopoulos, S., Dinoi, A., Donateo, A., Giannaros, C., Gregoris, E., Karagiannidis, A., Konstandopoulos, A. G., Ivosevic, T., Liora, N., Melas, D., Mifka, B., Orlic, I., Poupkou, A., Sarovic, K., Tsakis, A., Giua, R., Pastore, T., Nocioni, A., and Contini, D.: Atmospheric impact of ship traffic in four Adriatic-Ionian port-cities: Comparison and harmonization of different approaches, Transportation Research Part D-Transport and Environment, 50, 431-445, 10.1016/j.trd.2016.11.016, 2017.

Moldanova, J., Fridell, E., Winnes, H., Holmin-Fridell, S., Boman, J., Jedynska, A., Tishkova, V., Demirdjian, B., Joulie, S., Bladt, H., Ivleva, N. P., and Niessner, R.: Physical and chemical characterisation of PM emissions from two ships operating in European Emission Control Areas, Atmospheric Measurement Techniques, 6, 3577-3596, 10.5194/amt-6-3577-2013, 2013.

Murphy, S. M., Agrawal, H., Sorooshian, A., Padró, L. T., Gates, H., Hersey, S., Welch, W. A., Lung, H., and Miller, J. W.: Comprehensive simultaneous shipboard and airborne characterization of exhaust from a modern container ship at sea, Environmental Science & Technology, 43, 4626-4640, 2009.

Petzold, A., Hasselbach, J., Lauer, P., Baumann, R., Franke, K., Gurk, C., Schlager, H., and Weingartner, E.: Experimental studies on particle emissions from cruising ship, their characteristic properties, transformation and atmospheric lifetime in the marine boundary layer, Atmospheric Chemistry and Physics, 8, 2387-2403, 10.5194/acp-8-2387-2008, 2008.

Song, X. H., Hopke, P. K., Fergenson, D. P., and Prather, K. A.: Classification of single particles analyzed by ATOFMS using an artificial neural network, ART-2A, Analytical Chemistry, 71, 860-865, 10.1021/ac9809682, 1999.

Spencer, M. T., Shields, L. G., Sodeman, D. A., Toner, S. M., and Prather, K. A.: Comparison of oil and fuel particle chemical signatures with particle emissions from heavy and light duty vehicles, Atmospheric Environment, 40, 5224-5235, 10.1016/j.atmosenv.2006.04.011, 2006.

Toner, S. M., Sodeman, D. A., and Prather, K. A.: Single particle characterization of ultrafine and accumulation mode particles from heavy duty diesel vehicles using aerosol time-of-flight mass spectrometry, Environmental Science & Technology, 40, 3912-3921, 10.1021/es051455x, 2006.

Ulbrich, I. M., Canagaratna, M. R., Zhang, Q., Worsnop, D. R., and Jimenez, J. L.: Interpretation of organic components from Positive Matrix Factorization of aerosol mass spectrometric data, Atmospheric Chemistry and Physics, 9, 2891-2918, 2009.

Viana, M., Amato, F., Alastuey, A., Querol, X., Moreno, T., Garcia Dos Santos, S., Dolores Herce, M., and Fernandez-Patier, R.: Chemical Tracers of Particulate Emissions from Commercial Shipping, Environmental Science & Technology, 43, 7472-7477, 10.1021/es901558t, 2009.

Viana, M., Hammingh, P., Colette, A., Querol, X., Degraeuwe, B., de Vlieger, I., and van Aardenne, J.: Impact of maritime transport emissions on coastal air quality in Europe, Atmospheric Environment, 90, 96-105, 10.1016/j.atmosenv.2014.03.046, 2014.

Wenzel, R. J., Liu, D. Y., Edgerton, E. S., and Prather, K. A.: Aerosol time-of-flight mass spectrometry during the Atlanta Supersite Experiment: 2. Scaling procedures, Journal of Geophysical Research-Atmospheres, 108, 8427 10.1029/2001jd001563, 2003.

Xiao, Q., Li, M., Liu, H., Deng, F., Fu, M., Man, H., Jin, X., Liu, S., Lv, Z., and He, K.: Characteristics of marine shipping emissions at berth: profiles for PM and VOCs, Atmos. Chem. Phys. Discuss., 2018, 1-29, 10.5194/acp-2017-1132, 2018.

Yang, D.-q., Kwan, S. H., Lu, T., Fu, Q.-y., Cheng, J.-m., Streets, D. G., Wu, Y.-m., and Li, J.-j.: An Emission Inventory of Marine Vessels in Shanghai in 2003, Environmental Science & Technology, 41, 5183-5190, 10.1021/es061979c, 2007.

Zhang, Y., Yang, X., Brown, R., Yang, L., Morawska, L., Ristovski, Z., Fu, Q., and Huang, C.: Shipping emissions and their impacts on air quality in China, Science of the Total Environment, 581, 186-198, 10.1016/j.scitotenv.2016.12.098, 2017.

Zhao, M., Zhang, Y., Ma, W., Fu, Q., Yang, X., Li, C., Zhou, B., Yu, Q., and Chen, L.: Characteristics and ship traffic source identification of air pollutants in China's largest port, Atmospheric Environment, 64, 277-286, 10.1016/j.atmosenv.2012.10.007, 2013.

Figures

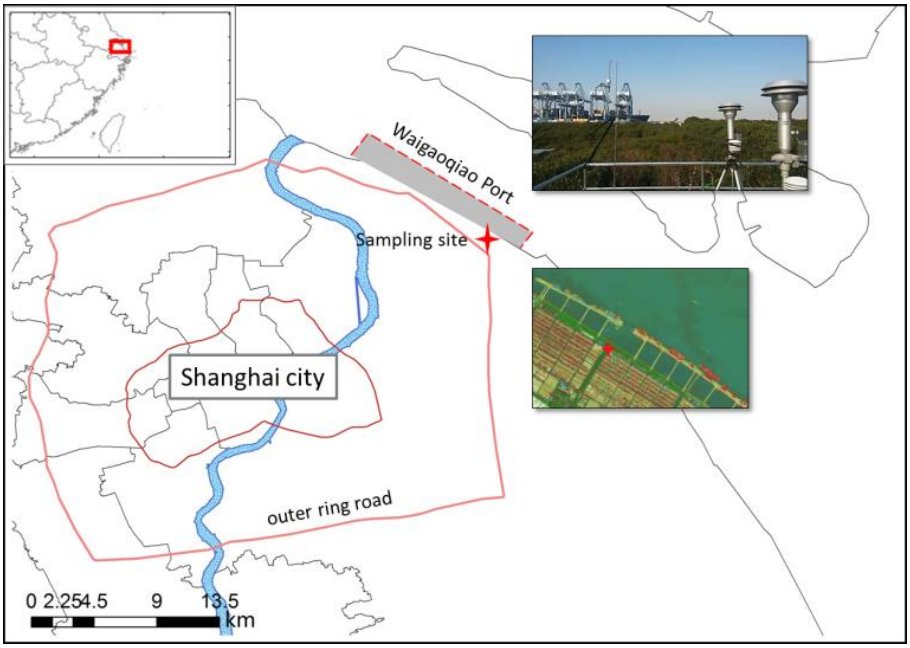

Figure 1: Map of sampling site in Shanghai port and surrounding areas. Port region is indicated by shaded area. The insets are the satellite image of the port site and a photo taken on the roof of monitoring station seeing in port direction.

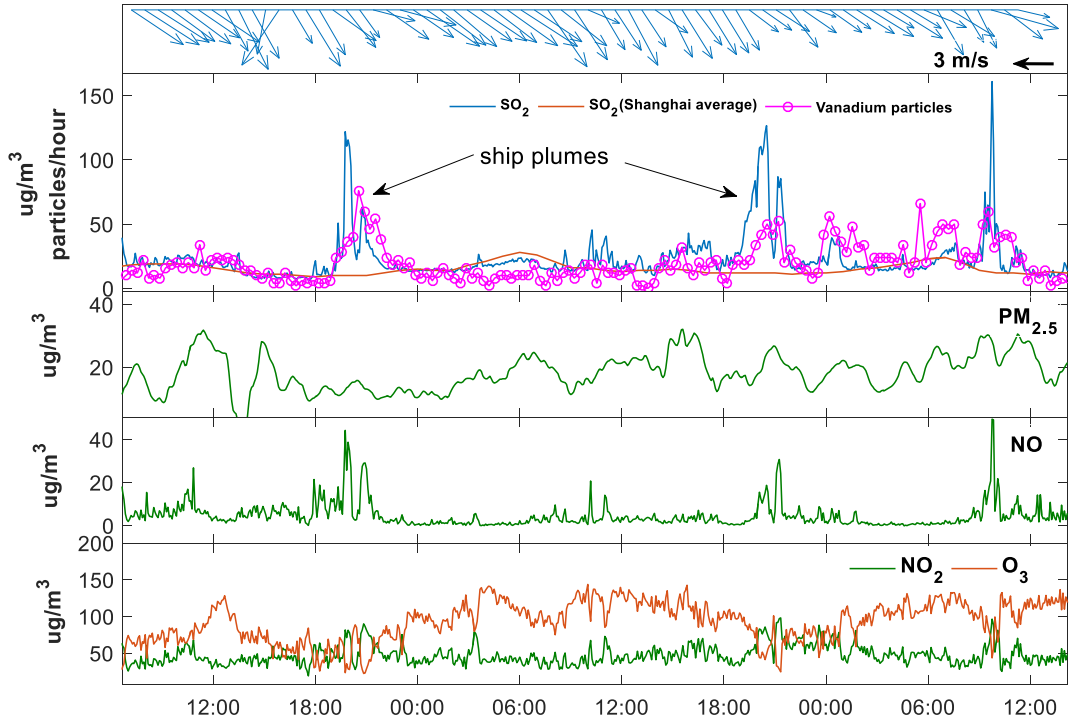

Figure 2: Temporal concentration of pollutants SO_2, NO, NO_2, O_3 and PM2.5 during 27-29 August 2016. Contemporary wind direction and speed, SO2 concentration of Shanghai city and vanadium particles number concentration as detected by SPAMS are included as a reference.

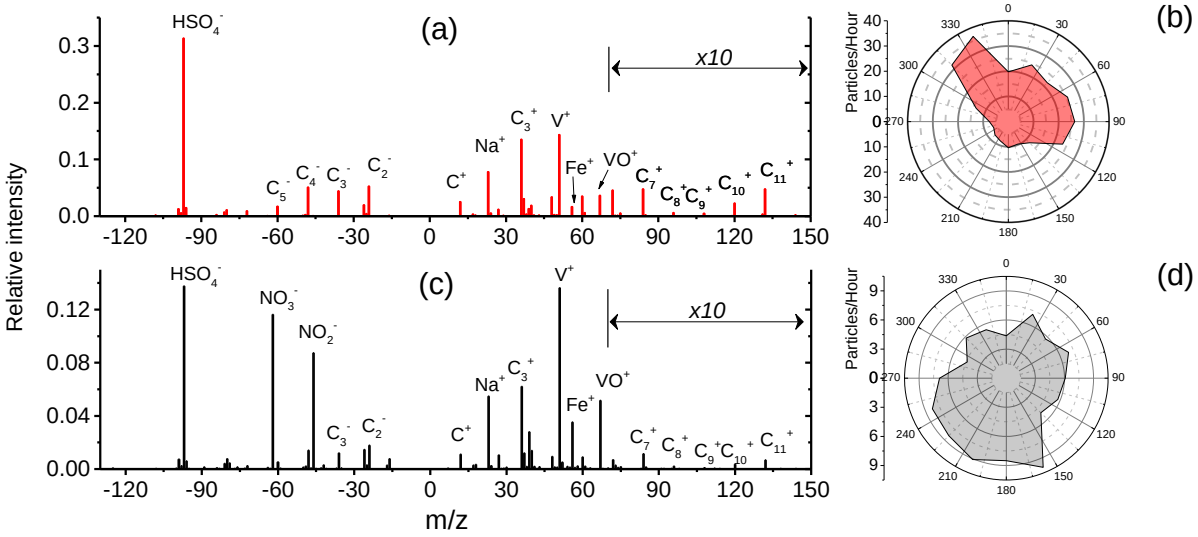

Figure 3: Mean mass spectra of fresh and background ship emission particles in port (a, c) and the wind rose of particle number concentration (in measure of particle number per hour) of these two particle types (b, d). Peaks in mass range of 70-150 in (a) and (c) are magnified by 10 times.

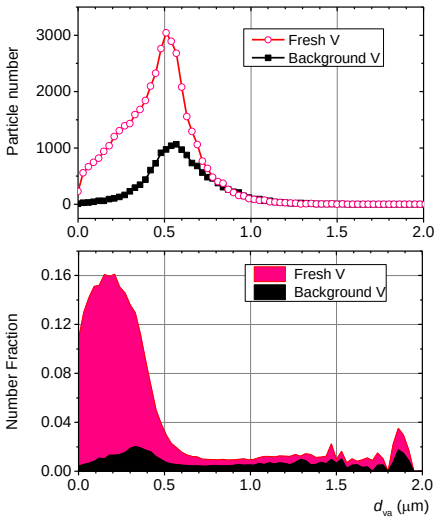

Figure 4: Particle number size distribution of fresh and background ship emission particles by SPAMS (Upper). Size distribution of these fresh and background types of ship emission particles normalized by total particles at each size (Lower).

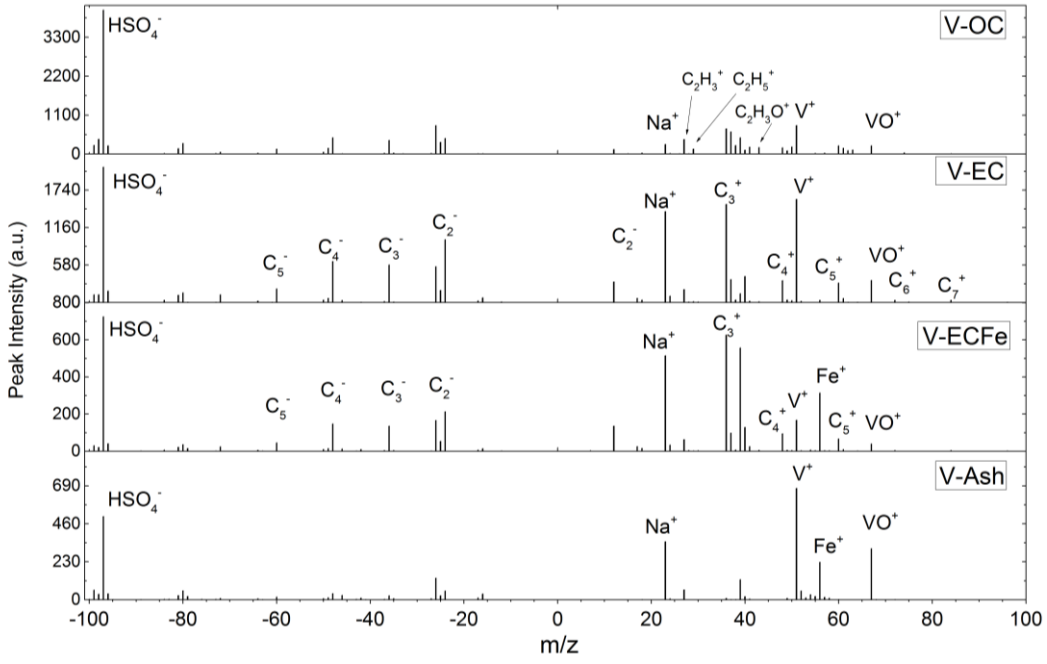

Figure 5: Mean mass spectra of four major particle types from fresh ship emission.

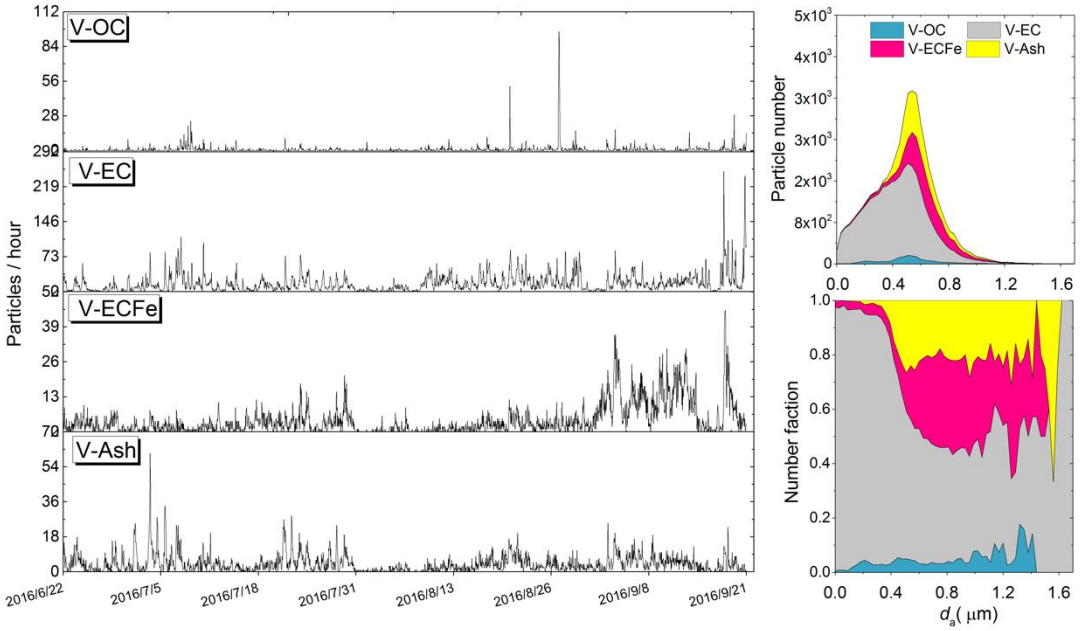

Figure 6: Temporal trend of number concentrations of four fresh vanadium particle types (Left panel); the number (upper right) and number fraction (lower right) of four vanadium particle types as a function of particle size.

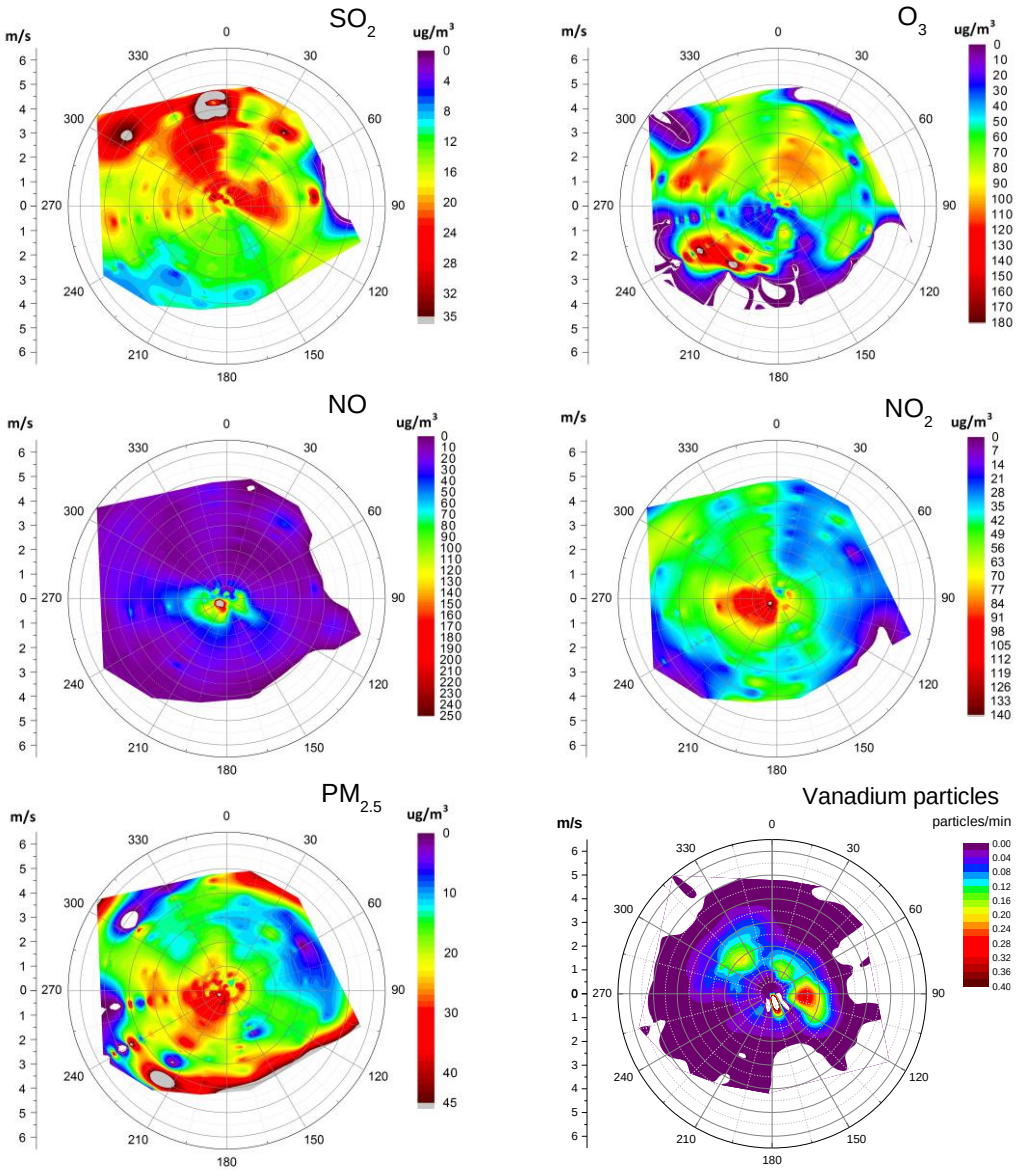

Figure 7: Pollution roses of SO_2, NO, NO_2, O_3, $PM_{2.5}$ and vanadium particles during the whole study period. Vanadium particles wind rose is based on number concentration as measured by SPAMS.

Tables.

Table 1: Statistics of pollutants concentration level during the whole sampling period. Numbers are average concentration followed by 25th and 75th quantiles in brackets. Average pollution levels in Shanghai city during the same period are included as a comparison.

	In plume		Non-plume		Non-plume (port sector)		Port average		Shanghai average	
SO_2 ($\mu g/m^3$)	**28.3**	(17.6~31.8)	**9.9**	(8.1~11.6)	**10.2**	(8.2~12.1)	**15.6**	(8.7~16.8)	**10.8**	(9~12)
NO ($\mu g/m^3$)	**42.5**	(7.6~47.5)	**41.6**	(7.1~59.1)	**16.5**	(1.8~18.1)	**41.9**	(7.3~55.3)	**5.8**	(3~6)
NO_2 ($\mu g/m^3$)	**59.3**	(36.1~72.4)	**50.5**	(27.8~60.8)	**36.9**	(22.1~46.1)	**53.2**	(30.3~65.0)	**30.2**	(18~38)
O_3 ($\mu g/m^3$)	**53.1**	(19.3~77.8)	**54.6**	(15.4~84.7)	**71.3**	(45.4~97.6)	**54.1**	(16.9~82.7)	**81.1**	(40~107)
$PM_{2.5}$ ($\mu g/m^3$)	**30.2**	(14.8~39.6)	**25.1**	(12.8~32.5)	**19.6**	(11.6~23.2)	**26.7**	(13.2~34.1)	**31.4**	(16~43)
Vanadium particles (#/hour)	**47.6**	(31~55)	**10.9**	(5~17)	**12.3**	(7~19)	**22.8**	(7~29)	---	

Table 2: Contributions of ship emissions to ambient pollutants SO_2, NO, NO_2, O_3, $PM_{2.5}$ and vanadium particles in port area. Calculations are based on two situations: entire sampling period (all wind directions included) and only when site is in downwind direction of port emissions. Total lengths (in hours) of respective periods are given.

(%)		In port sector (excluding land-based emissions)		Entire period (including land-based emissions)	
		Average	range	Average	range
SO_2		57.2	(49.2, 64.8)	36.4	(29.2, 40.2)
NO		71.9	(57.0, 84.6)	0.7	(0.2, 1.7)
NO_2		30.4	(24.7, 34.6)	5.1	(3.7, 7.9)
O_3		-16.6	(-18.8, -13.4)	-0.9	(-2.8, -0.4)
$PM_{2.5}$		27.6	(22.5, 33.2)	5.9	(3.4, 9.6)
Vanadium particles*	(0-0.4μm)	79.2	(73.9, 85.0)	57.1	(50.6, 64.0)
	(0.4-0.8μm)	75.3	(68.1, 82.0)	44.7	(38.1, 52.3)
	(0.8-2.5μm)	76.6	(70.4, 82.9)	47.0	(41.3, 52.9)
	(0-2.5μm)	77.0	(70.6, 83.1)	49.5	(43.0, 56.7)

Length of sampling (in hours): Entire period: 2256; Port sector: 1136; In plume: 694;Non-plume: 1563; Non-plume (port sector): 625.
* Particle number contribution